



ELSEVIER

Journal of Atmospheric and Solar-Terrestrial Physics ■ (■■■■) ■■■-■■■

**Journal of
ATMOSPHERIC AND
SOLAR-TERRESTRIAL
PHYSICS**

www.elsevier.com/locate/jastp

Mean and variable forcing of the middle atmosphere by gravity waves

David C. Fritts*, Sharon L. Vadas, Kam Wan, Joseph A. Werne

Colorado Research Associates, a Division of NorthWest Research Associates, 3380 Mitchell Lane, Boulder, CO 80301, USA

Abstract

Recently we have begun to appreciate more fully the degree and the consequences of variability in gravity wave (GW) forcing of the middle atmosphere. Such variability arises for a number of reasons. GW sources in the lower atmosphere reflect the significant spatial and temporal variability of normal meteorological processes. GW amplitudes and characteristics are modulated by the wind and temperature fields through which they propagate. Nonlinear interactions and instability processes impose or amplify variability in energy and momentum transport and deposition. Finally, variability appears to be greatest among GWs occurring at the smaller spatial scales and periods that account for the majority of energy and momentum transports into the middle atmosphere. This paper both surveys recent findings and introduces new results.

© 2005 Elsevier Ltd. All rights reserved.

Keywords: Gravity waves; Middle atmosphere dynamics; Instability dynamics; Turbulence

1. Introduction

We have known for many years that gravity wave (GW) amplitudes and characteristics exhibit considerable variability in the lower and middle atmosphere. The dominant sources in the lower atmosphere, including convection, orography, and wind shear, all yield GWs having spatial and temporal scales reflecting source characteristics because GW excitation can often be viewed as a linear or quasi-linear response to what is often a highly nonlinear process. The various sources of GWs in the middle atmosphere, and the GW characteristics arising from them, were recently

reviewed in some detail by Fritts and Alexander (2003). It is generally believed, for example, that both the spatial scales and temporal behavior of convection and the environmental shears in which convection occurs contribute to the characteristics and anisotropy of the resulting GW field. Orography also leads most often to a linear GW response that reflects the spatial scales and orientation of the terrain. Wind shear, in contrast, may favor excitation via a nonlinear mechanism, so-called “envelope” radiation, because the linear growth rates of the larger horizontal scales that can propagate vertically away from the shear are much smaller than the growth rates of the smaller-scale Kelvin–Helmholtz (KH) instability that itself imposes the envelope (or packet) scale. Other source mechanisms are also operative, including frontal dynamics and adjustment processes, and contribute to the

*Corresponding author. Tel.: +1 303 415 9701x205; fax: +1 303 415 9702.

E-mail address: dave@co-ra.com (D.C. Fritts).

1 GW spectrum over a wide range of scales, but these
 2 have not been studied as extensively to date (see
 3 [Fritts and Alexander, 2003](#)).

4 Once excited, GWs propagate through an atmo-
 5 sphere that itself exhibits variability on all possible
 6 spatial and temporal scales. Over a large range of
 7 scales, ~ 1 –1000 km and a few minutes to tens of
 8 hours, this variability is imposed by the GW
 9 spectrum itself. Variability at smaller and larger
 10 scales accompanies turbulence arising most often
 11 from GW instability processes (and convection at
 12 lower altitudes) and planetary-scale motions (tides
 13 and planetary waves). A variable environment
 14 contributes both coherent (systematic) and incoher-
 15 ent (random) variations in GW properties, with the
 16 coherent responses determined to a large extent by a
 17 linear dispersion relation (and ray equations)
 18 relating GW phase speeds (or intrinsic frequencies)
 19 and wavenumbers to environmental density, strati-
 20 fication, winds, and shears. GW scales range from
 21 horizontal wavelengths of ~ 10 –1000 km and verti-
 22 cal wavelengths of ~ 1 –100 km and intrinsic fre-
 23 quencies range from the inertial to the buoyancy
 24 frequency, with both the vertical wavelength and the
 25 intrinsic frequency determined initially by source
 26 conditions and thereafter by the GW propagation
 27 environment. Of greatest relevance in this paper are
 28 the variations that occur in intrinsic phase speed (or
 29 vertical wavenumber) and vertical group velocity,
 30 since GWs attaining large amplitudes and high
 31 vertical group velocities can dominate GW influ-
 32 ences at greater altitudes.

33 Nonlinear dynamics occurring within a GW field
 34 also contribute to, and may indeed amplify,
 35 variability arising from linear dynamics alone. This
 36 is because all GWs are inherently unstable to a wide
 37 range of perturbations. At smaller amplitudes, these
 38 instabilities manifest as systematic exchanges of
 39 energy among GWs exhibiting weak “resonant”
 40 interactions ([Klostermeyer, 1991](#); [Vanneste, 1995](#);
 41 [Sonmor and Klaassen, 1997](#)) that are believed not
 42 to impact GW momentum transport. At larger
 43 amplitudes, however, these instabilities lead to GW
 44 dissipation, breaking, turbulence, spectral energy
 45 transfers, and divergent momentum fluxes that play
 46 prominent roles in middle atmosphere dynamics
 47 ([Fritts, 1984a, 1989](#); [Dunkerton, 1987, 1989](#); [Son-
 48 mor and Klaassen, 1997](#); [Fritts and Alexander,
 49 2003](#)). Instability dynamics also impose both mean
 50 and spatially and temporally localized flux diver-
 51 gence that forces the zonal mean circulation and
 excites additional GWs at higher altitudes ([Fritts et](#)

[al., 2003](#); [Vadas and Fritts, 2001](#); [Vadas et al.,
 2003](#)). 53

54 The purpose of this paper is to review and update
 55 our understanding of the causes and effects of mean
 56 and variable GW forcing of the middle atmosphere.
 57 Characteristics and influences arising from various
 58 GW sources are described in Section 2. These
 59 suggest very different influences by different
 60 sources, both in GW character and in their
 61 geographic and temporal distributions. Propagation
 62 effects and contributions to forcing variability are
 63 discussed in Section 3. These provide several
 64 mechanisms by which localized GW forcing can
 65 arise. Section 4 reviews the implications of nonlinear
 66 interaction and instability processes for mean and
 67 variable GW forcing. Nonlinear processes are likely
 68 the least quantified at this time; we are, neverthe-
 69 less, beginning to understand the range of important
 70 dynamics in a qualitative manner. Our results are
 71 summarized in Section 5. 73

2. GW source characteristics 75

76 This section reviews GW character and variability
 77 due to the dominant GW sources as we understand
 78 them at present. As noted above, the sources we
 79 believe to dominate GW excitation in the lower
 80 atmosphere are convection, orography, and wind
 81 shear, though these vary with geography, season,
 82 and local meteorology. Other sources are also
 83 important under certain conditions and/or for
 84 specific portions of the GW spectrum. These include
 85 frontal dynamics, adjustment of unbalanced flows,
 86 wave–wave interactions, local body forcing (effec-
 87 tively the local acceleration accompanying GW
 88 dissipation and momentum flux divergence), and a
 89 few others likely less important. 91

2.1. Convection 91

92 Both satellite and balloon studies have revealed
 93 that GW variances are largest throughout the
 94 stratosphere at equatorial latitudes ([Fetzer and
 95 Gille, 1994, 1996](#); [Allen and Vincent, 1995](#); [Tsuda
 96 et al., 2000](#); [Alexander et al., 2000](#)). This appears to
 97 be largely a result of the importance of deep
 98 convection as a major source of GWs and the
 99 presence of most deep convection in the tropics
 100 ([Salby and Garcia, 1987](#); [Taylor and Hapgood,
 101 1988](#); [Fritts and Nastrom, 1992](#)). It has also been
 102 argued, however, that the large mean variances at
 103 tropical latitudes are due, in part at least, to an

1 observational bias favoring the detection of slow
moving inertia-GWs (Alexander et al., 2002).

3 Deep, fast convection excites GW having large
vertical scales and high intrinsic frequencies and
5 phase speeds (Fovell et al., 1992; Dewan et al., 1998;
Piani et al., 2000; Lane et al., 2001; Horinouchi et
7 al., 2002; Sentman et al., 2003; Vadas and Fritts,
2004). Mesoscale convective complexes (MCC) that
9 also organize convection on much larger scales,
however, and additionally excite considerable GW
11 activity near inertial frequencies that may have
significant influences to high altitudes (Pfister et al.,
13 1986; Tsuda et al., 1994; Karoly et al., 1996;
Shimizu and Tsuda, 1997; Garcia and Sassi, 1999;
15 Wada et al., 1999; Vincent and Alexander, 2000).

Three mechanisms are thought to describe
17 approximately GW generation by convection. These
are (1) thermal forcing via latent heat release that
19 excites vertical scales comparable to the forcing
depth (Bergman and Salby, 1994; Alexander et al.,
21 1995; Piani et al., 2000), (2) the “obstacle” or
“transient mountain” effect in which wind shear at
23 cloud top imposes relative motion over convective
cells (Clark et al., 1986; Pfister et al., 1993a, b;
25 Alexander and Vincent, 2000; Vincent and Alex-
ander, 2000), and (3) a “mechanical oscillator”
27 effect in which oscillatory convective plumes project
those periods onto the GW field (Fovell et al., 1992;
29 Lane et al., 2001). More recently, Lane and Clark
(2002) revisited the convective boundary layer
31 problem and concluded that GWs were excited
primarily by oscillatory motions with GW struc-
33 tures determined largely by filtering thereafter. The
relative importance of heat and momentum flux
35 convergence and diabatic forcing was also examined
by Song et al. (2003). They concluded that forcing
37 by net flux convergence is comparable to diabatic
heating, that these sources are largely out of phase,
39 and that the net effect is less efficient excitation of
GWs that are able to reach the stratosphere.

41 Other processes also operate to make convection
a highly variable GW source. Wind shear in the
43 troposphere yields tilted convection and GWs
having that same preferred phase tilt and direction
45 of propagation. While GW scales depend in large
part on the spatial scales of convection, the
47 temporal behavior poses an additional constraint,
essentially eliminating GW periods shorter than the
49 characteristic time scale of the convection (Vadas
and Fritts, 2004). The net effect convectively
51 generated GWs that span horizontal scales of
~10–1000 km and periods of minutes to 10’s of

53 hours, with the largest amplitudes, frequencies, and
momentum fluxes accompanying convection that is
55 deep, spatially localized, and fast (Piani et al., 2000;
Lane et al., 2001; Vadas and Fritts, 2004).

57 Examples of the GW patterns arising from an
analytic description of convective plumes and the
59 corresponding frequency and vertical wavenumber
spectrum exhibiting a range of spatial and temporal
61 scales are shown in Fig. 1 (Vadas and Fritts, 2004).
For these choices of source scales, the dominant
63 responses and momentum fluxes occur at horizontal
and vertical wavelengths of ~40 and 14 km and
65 periods of ~15 min (~3 buoyancy periods, T_b). The
forcing geometry and the character of the GWs
67 excited are shown in the left panel of Fig. 2. Deep
and relatively narrow sources lead to GWs having
69 large vertical scales and steep phase slopes. Because
such motions also have high phase speeds and
71 vertical group velocities, they may penetrate to high
altitudes in a variety of environments. It is
73 important to note, however, that those GWs that
achieve very high altitudes have similar frequencies
75 ($\omega \sim N/3$) but significantly larger spatial scales,
horizontal and vertical wavelengths of ~100 and
77 40 km, respectively (see Vadas and Fritts, 2004).

2.2. Orography 79

81 GW generation by orography has been studied
extensively because such waves have effects
83 throughout the atmosphere. At lower altitudes,
mountain waves may induce strong local flows
85 and wave drag that influence surface flows and
tropospheric jet structure and are important for
87 numerical modeling of tropospheric weather. But
GWs generated by orography may also penetrate to
89 much greater altitudes and influence the local and
zonal mean structures of the stratosphere, meso-
91 sphere, and lower thermosphere (Pruesse et al.,
2002; Jiang et al., 2002, 2003, 2004; Kim et al., 2003;
93 Fritts and Alexander, 2003). Mountain wave forcing
is often approximately linear, though strong non-
95 linear, or resonant, responses (downslope or “chi-
nook” winds) may develop on the lee slope when
97 atmospheric structure is suitable. Such forcing also
varies strongly with terrain height, scale, and
99 orientation. Flow may be around rather than over
terrain if the Froude number, $Fr = U/Nh$, is small
101 or the terrain is three-dimensional (3D) or aligned
along the flow; the flow may also separate from the
103 terrain, leading to much smaller GW responses. Like
convection, orography excites GWs having a

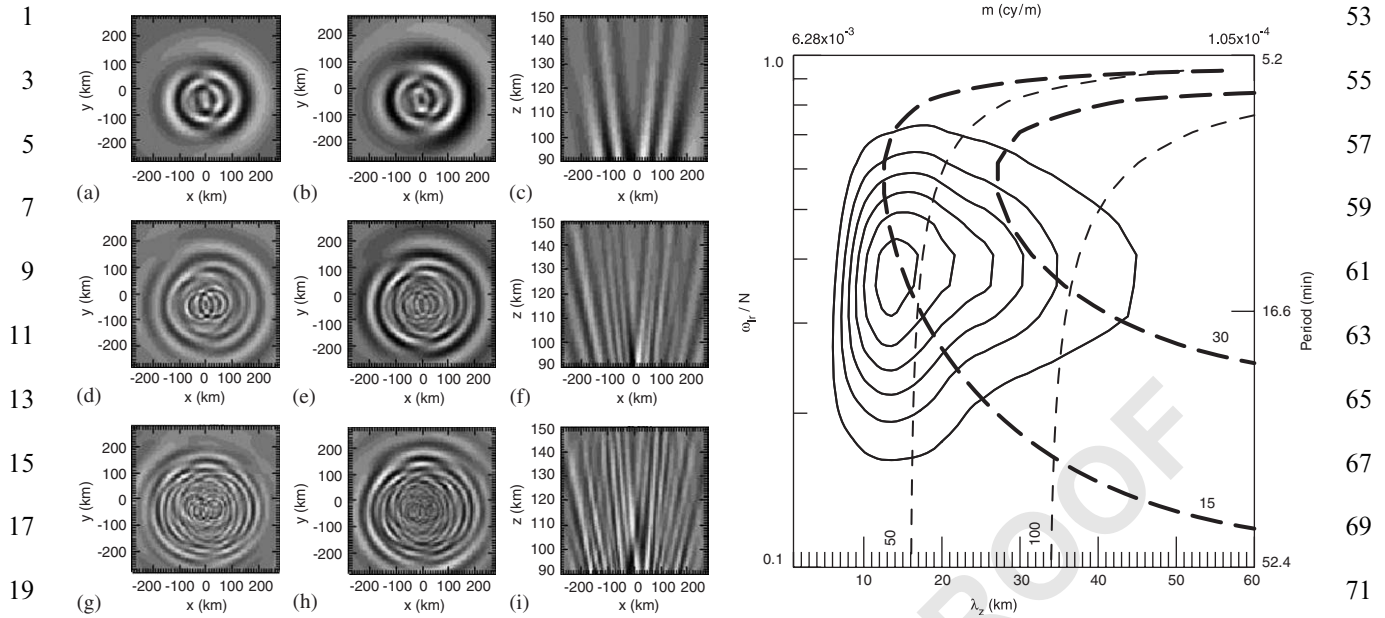


Fig. 1. GW patterns in vertical velocity and perturbation temperature (left and center cross sections) at 90 km and vertical velocity from 90 to 150 km (right cross sections) above a simulated mesoscale convective complex (MCC). The corresponding distribution of GW energy with vertical wavelength and intrinsic frequency arising from a cluster of convective plumes with mean widths and depths of ~ 5 – 10 km and ~ 1.5 – 6 km, respectively (see Vadas and Fritts, 2004, for further details).

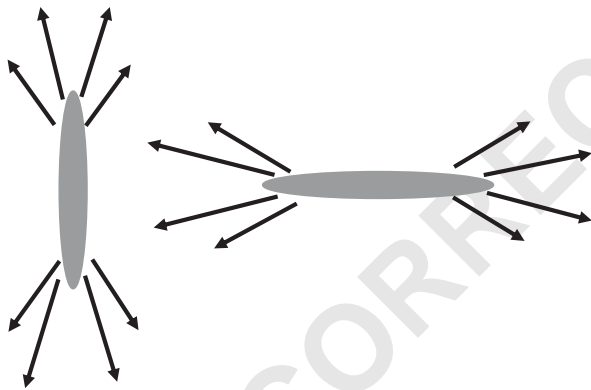


Fig. 2. Body force geometries and associated GW ray paths for a deep, narrow vertical forcing representative of convective plumes (left) and a shallow, horizontally extensive horizontal forcing more typical of a slow adjustment process (right). In each case, the spatial scales largely determine the frequencies of the radiated GWs, except that the forcing time scale may further restrict the excitation of high frequencies.

wide range of spatial scales and intrinsic frequencies, with the dominant fluxes and effects accompanying waves having large amplitudes, small scales, and high intrinsic frequencies. But unlike convection, mountain waves have phase speeds near

zero and thus penetrate to high altitudes only when sufficiently nonzero winds (along the plane of propagation) extend throughout the atmospheric column, a process that appears to occur at only a few preferred sites (Jiang et al., 2002; Pruesse et al., 2002). While 3D orography induces 3D GW propagation (Broutman et al., 2002, 2003, 2004), the dominant momentum fluxes are associated with GWs propagating upstream relative to the local mean flow exciting the GW response.

2.3. Wind shear

Wind shear is believed to be a statistically significant source of GWs near the tropopause and at higher altitudes, based on modeling and observational studies. Modeling has suggested that the most likely source mechanism may be envelope radiation, as linear growth of larger-scale GWs cannot compete with that of the KH instability (Fritts, 1984b; Chimonas and Grant, 1984; Scinocca and Ford, 2000; Bühler et al., 1999). Other studies have revealed enhanced variances in the vicinity of jet stream shears or argued that such a source is likely to contribute significantly to the momentum budget of the middle atmosphere (Fritts and Nastrom,

1992; Bühler and McIntyre, 1999). Thus, while we believe that wind shear is likely an important source, this source is more poorly understood and quantified than convection and orography at this time. We do know, however, that phase speeds must be comparable to mean winds at the source altitude (from the Miles-Howard semi-circle theorem). We suspect that such forcing leads to horizontal scales that are 10's rather than hundreds or thousands of km because KH patches appear nearly always to be limited in their horizontal extent (Fritts and Alexander, 2003; Hecht et al., 2004). Finally, we know that such a nonlinear process is highly intermittent because it results from the exponential growth of KH shear instability, in which KH growth and turbulent breakdown occupies only a few T_b (Palmer et al., 1996; Fritts et al., 1996a; Werne and Fritts, 1999).

2.4. Adjustment processes

Adjustment processes of unbalanced flows encompass a wide range of approximations and dynamics (McIntyre, 2003). The most simplistic of these is an imbalance at some order of approximation that arises either from an initial unbalanced state (Rossby adjustment) or as the large-scale flow evolves from (or is perturbed from) a balanced to an unbalanced state ("spontaneous" adjustment) (see McIntyre, 2003). In general problems, this adjustment involves alteration of the 3D wind and geopotential fields to attain a new balanced state and the radiation of inertia-GWs (IGWs) to accommodate energy and momentum conservation. Spatial and temporal scales for such processes can vary widely, with spontaneous adjustment of large-scale flows (such as jet structures or troposphere-stratosphere exchange events) occurring on scales of hundreds or thousands of km and many hours. At the other end of the spectrum, instability dynamics, specifically shear instability and GW breaking, can result in small-scale flows (10's of km or less) that evolve to an unbalanced state on time scales of an hour or less.

Large-scale adjustment processes having long time scales are illustrated schematically in the right panel of Fig. 2, with emergence of IGWs having large horizontal scales, much smaller vertical scales (because jet streams are much thinner than they are wide), and a dominance of intrinsic frequencies near the inertial frequency (Fritts and Luo, 1992; Luo and Fritts, 1993; Vadas and Fritts, 2001). Smaller-

scale adjustment processes can exhibit a wide range of spatial and temporal scales, depending on the geometry and the time scale of the event. For example, rapid events can be triggered by rearrangement of the local wind and temperature structure due to KH shear instability (Bühler et al., 1999) occurring on spatial scales of $\sim 1-10$'s of km and time scales of a few T_b (Werne and Fritts, 1999; Fritts and Alexander, 2003) or to the body forcing (see below) accompanying GW momentum flux divergence in a local breaking event. In all cases, however, the resulting GW scales are determined by a combination of event spatial and temporal scales.

A deep, narrow, fast event will lead to GW excitation resembling the left panel in Fig. 2. A wide, shallow event (right panel of Fig. 2) will lead to IGW excitation only, independent of whether the time scale is fast or slow, because the source has no spatial components having steep phase slopes. In cases where the event spatial scales are deep and narrow, but the time scales are long, there is a mismatch between the intrinsic frequencies implied by the spatial geometry and the slow evolution of the flow, and the radiation of high-frequency GWs is suppressed (Lighthill, 1978, Section 4.9; Vadas and Fritts, 2001). Indeed, as the time scale for adjustment becomes very long, GW radiation becomes negligible, but the new balanced mean state is independent of the time scale of the adjustment (Vadas and Fritts, 2001; Bühler and McIntyre, 2005). The IGW field and two-dimensional (2D) wavenumber-frequency spectrum arising from spontaneous adjustment having Gaussian geometry, a length, width, and depth of 500, 100, and 2 km (full-width, half-maximum, FWHM), respectively, and a time scale of 1 h (FWHM) is shown for comparison with the response to deep, fast forcing in Fig. 3. The results displayed here employed a Fourier-Laplace transform that represents an exact solution of the linear Boussinesq equations (Vadas and Fritts, 2001).

2.5. Local body forces

The role of localized GW breaking as a source of middle atmosphere variability and additional GWs having significant influences at higher altitudes is likely under-appreciated at present. However, the tendencies (1) for sources of high-frequency GWs to be spatially localized, intermittent, and strong, (2) for GWs having large-amplitudes and large momentum fluxes to also be spatially localized at

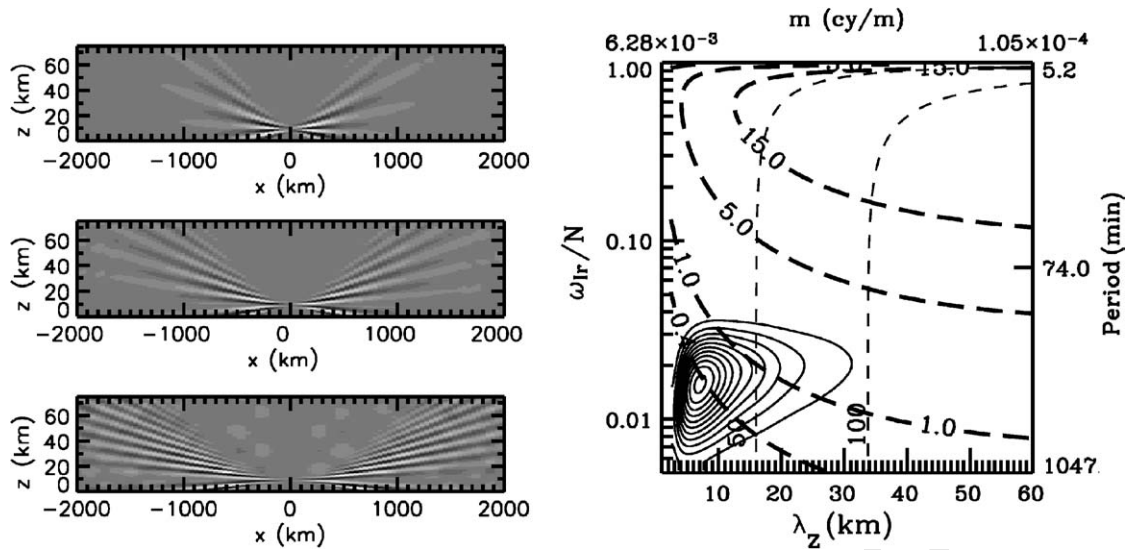


Fig. 3. GW radiation resulting from spontaneous adjustment of a zonal jet centered at 10 km and having Gaussian cross sections with FWHM dimensions of 500, 100, and 2 km in (x, y, z) , respectively, and a time scale of 1 h. Note the predominance of GWs having intrinsic frequencies of $\sim N/50$, corresponding to the scales imposed by the forcing geometry.

higher altitudes, and (3) for instability dynamics to lead to rapid, local breaking and momentum flux divergence (see below) together suggest that GW forcing of the large-scale flow is more likely to be intermittent and variable than smooth, systematic, and uniform. Thus, while the mean response to GW forcing is the same whether forcing is uniform or highly variable in time (apart, perhaps, from influences of larger-scale wave motions and filtering, see below), local GW instability, momentum flux divergence, and forcing are likely an increasingly important source of additional GWs at higher altitudes.

GWs arise from wave breaking regions in two ways. One is via direct nonlinear interactions that excite other GWs at smaller scales (or higher harmonics) of the parent GW (see below). The second is via the adjustment process accompanying rapid, local body forcing due to local instability and momentum flux divergence and has been addressed by Zhu and Holton (1987), Vadas and Fritts (2002), and Vadas et al. (2003). As discussed above, the spatial scales and intrinsic frequencies of the resulting GWs depend on the spatial and temporal scales of the body forcing event, but it is noteworthy that deep, rapid instability processes can lead to GWs having significantly larger scales and vertical group velocities than the GW undergoing instability. In such cases, the radiated GWs may penetrate to, and have influences at, very much higher

altitudes than the initial GW itself. One additional caveat that is important to note is the requirement that the time scale for initial GW propagation, essentially its period, be shorter than the time scale of the radiated GWs, for the same reasons as discussed for adjustment processes above (Bühler and McIntyre, 2005).

An example of an apparent strong local GW breaking and body forcing event seen in the OH airglow emission by Yamada et al. (2001) and diagnosed by Fritts et al. (2002) is shown in Fig. 4. This event occurred on horizontal and vertical scales of ~ 50 and 10–20 km, a time scale of a few T_b (~ 10 min or less), and accompanied a GW having a high intrinsic frequency, a large vertical wavelength, and attaining a very large amplitude prior to instability. The estimated spectrum of radiated GWs was found to be qualitatively like that shown in Fig. 1, seeming to confirm the potential importance of such instability events as another source of GWs at higher altitudes.

2.6. Other sources

Additional GW sources likely to be important in the lower and middle atmosphere include frontal dynamics and wave–wave interactions. Others likely play a smaller role. Frontogenesis leads to IGW excitation because of the large horizontal scales involved (Griffiths and Reeder, 1996; Reeder and

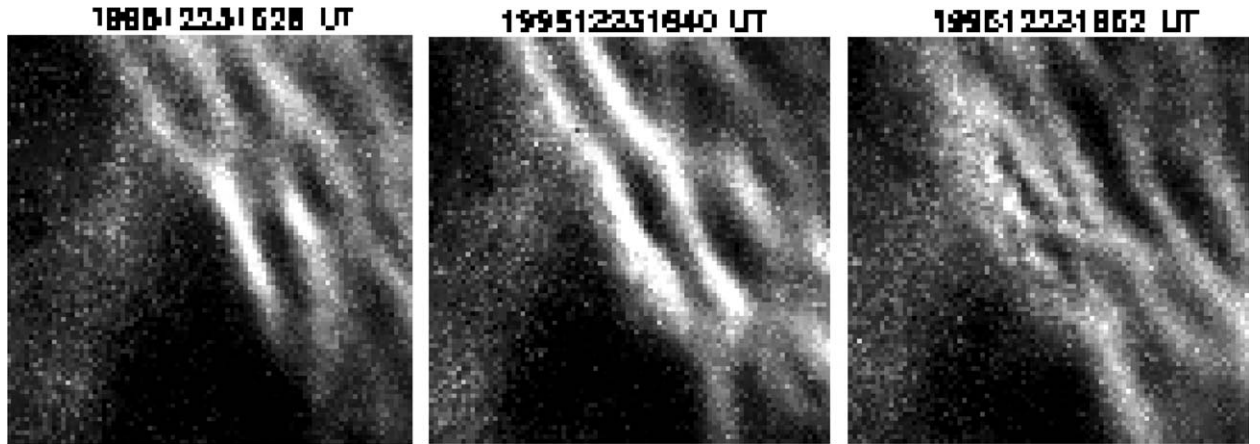


Fig. 4. GW structure in OH airglow showing wave amplification and instability. Successive images are spaced by 4 and 12 min, intensity perturbations achieved values as large as 55%, and temperature perturbations were $\sim 10\%$ prior to breaking (after Yamada et al., 2001). The GW horizontal wavelength was ~ 27 km and the spatial scale of the breaking region was inferred to be ~ 50 km horizontally and ~ 10 – 20 km vertically (Fritts et al., 2002).

Griffiths, 1996) and is very like jet stream adjustment as a source. Associated convection and instability dynamics may excite GWs at the other (higher) ends of the wavenumber and frequency spectra, as noted above. Wave–wave interactions operate across the full range of the GW spectrum and will be discussed further below.

2.7. GW energy and momentum flux spectra

Collectively, GW sources and interactions in the lower and middle atmosphere contribute to the establishment of a “mean” GW spectrum having near-universal shapes in frequency and wavenumber, despite many reasons to expect otherwise (VanZandt, 1982; Fritts and VanZandt, 1987, 1993; Tsuda et al., 1991; Nastrom et al., 1997; Fritts and Alexander, 2003). A schematic of the mean spectra of horizontal and vertical GW energy density with intrinsic frequency is shown in the left panel of Fig. 5 and emphasizes what we see in essentially all ground-based observations: GW energy density peaks near the inertial frequency and has a near-universal slope of $\sim -5/3$. Limited in situ measurements of the intrinsic frequency spectrum using constant-pressure balloons by Hertzog and Vial (2001), however, suggest a somewhat steeper slope of the intrinsic frequency spectrum of ~ -2 . The corresponding frequency distribution of momentum flux inferred from the energy spectra and the dispersion relation (and confirmed by multiple observations, see Fritts and Alexander, 2003) is shown in the right panel of Fig. 5. Note that

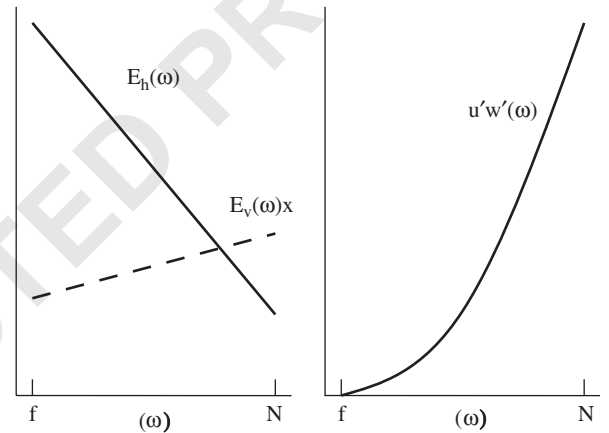


Fig. 5. Schematic of GW energy in horizontal and vertical motions (left) and the corresponding momentum flux (right) as functions of intrinsic frequency. Note that at middle and high latitudes, momentum flux is strongly concentrated at high intrinsic frequencies.

the momentum flux, representing both vertical transports of horizontal momentum and meridional transports of heat (relevant only for IGWs), may be written in the form

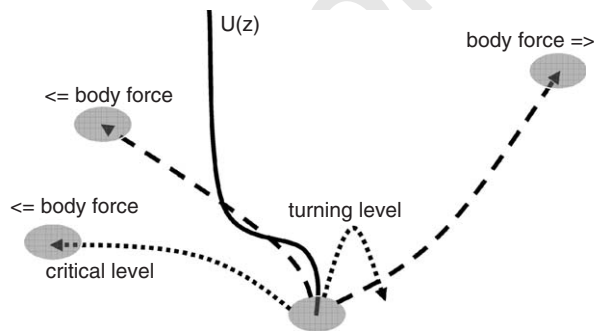
$$\overline{u'w'}(1 - f^2/\omega^2), \quad (1)$$

so that the two contributions exactly cancel at the inertial frequency (Andrews and McIntyre, 1976; Fritts and Alexander, 2003).

1 These energy and momentum flux spectra emphasize an important point that is often overlooked
 3 in assessing GW influences in the lower and middle atmosphere: dominant energies and momentum
 5 fluxes occur at *opposite ends* of the frequency spectrum. Thus the GWs having the largest
 7 amplitudes, energy densities, and horizontal scales (hence the most easily observable in many data sets)
 9 are *not* the GWs having the largest energy and momentum fluxes and atmospheric effects.

11 3. Influences of propagation

13 It is well known that GWs are strongly influenced by the environments through which they propagate.
 15 In most cases, this propagation can be described by approximately linear dynamics. There are, however,
 17 circumstances, especially for larger-amplitude GWs or for GWs in sheared and time-dependent environ-
 19 ments, where numerical studies suggest either significant departures from the expectations of
 21 linear theory or unusual behavior, GW responses, or structure (Broutman, 1986; Broutman and
 23 Young, 1986; Zhong et al., 1995; Broutman et al., 1997; Buckley et al., 1999; Sutherland, 1999, 2000,
 25 2001; Sonmor and Klaassen, 2000; Fritts and Alexander, 2003). Representative ray paths for
 27 GWs having varying initial intrinsic frequencies in a sheared environment are shown in Fig. 6. In this
 29 example, the mean wind profile exhibits a westward shear above the GW source which refracts GWs
 31 having both eastward and westward phase velocities. To understand linear GW propagation, we
 33 employ the approximate linear dispersion relation for GWs propagating in an east–west plane for



37 Fig. 6. Schematic showing GW propagation with ray paths from a localized source. Dashed lines show GWs that refract in the mean shear but maintain finite m^2 and propagate to higher altitudes before dissipating. Dotted lines show GWs that are excluded from higher altitudes due to a critical level encounter (left) and a turning level (right).

53 which rotational and shear effects are not important, which is given by

$$55 \quad m^2 = k^2(N^2/\omega^2 - 1) - 1/4H^2, \quad (2) \quad 57$$

59 where k and m are the horizontal and vertical wavenumbers, N the buoyancy frequency, $\omega = k(c - U)$ is the intrinsic frequency, c and U are the GW phase speed and mean wind in the direction of GW propagation, and H the density scale height, typically ~ 7 km. 63

65 GWs having eastward propagation experience increasing ω within the wind shear. Initial frequencies that cause N^2/ω^2 to become sufficiently small that m^2 falls below zero within the shear layer become evanescent at greater altitudes (they encounter a turning level) and reflect in the vertical. 69 Other GWs having larger initial m and shallower propagation paths also exhibit refraction to smaller m and higher intrinsic frequencies (steeper propagation angles), but maintain positive m^2 , continue their upward propagation, and induce an eastward body force where these GWs are dissipated. 75

77 GWs having westward propagation experience decreasing ω within the shear layer. In this case, initial frequencies for which the corresponding phase speed, c , is less negative than the maximum negative wind speed, ω becomes zero (where $c = U$) and the linear dispersion relation implies that the GW encounters a critical level and is trapped at this level. For GWs having larger negative phase speeds, ω remains finite, $c < U$ everywhere, and these GWs refract to smaller vertical scales and shallower propagation, but retain their upward propagation and apply a westward body force where they dissipate. 87

89 Departures from this simple picture arise for a number of reasons. Two of those that impact GW spectral evolution are time dependence and a component of vertical motion of the local mean flow. Together, these result in significantly different interactions among diverse scales of motions, and different implications for spectral energy transfers, than when these effects are neglected (Bruhwiler and Kaper, 1995; Zhong et al., 1995; Broutman et al., 1997; Eckermann, 1997; Walterscheid, 2000). GW transience and packet localization likewise have some interesting effects, among them GW instability accompanying “self-acceleration” and instability 101 and permanent mean-flow changes at large GW amplitudes during turning level encounters (Sutherland, 1999, 2000, 2001). 103

1 Finally, GWs are strongly modulated by tidal and
 2 planetary wave motions, leading to strong GW
 3 filtering (Walterscheid, 1981; Smith, 1996) and
 4 significant modulations of GW variances and
 5 momentum fluxes at tidal (Fritts and Vincent,
 6 1987; Wang and Fritts, 1991) and planetary wave
 7 periods (Thayaparan et al., 1995; Isler and Fritts,
 8 1996; Nakamura et al., 1997; Manson et al., 1998).
 9 These GW modulations lead, in turn, to feedbacks
 10 on tidal and planetary wave structures, but there is
 11 considerable uncertainty at this time, with the
 12 magnitude (and sign) of the effect dependent on
 13 the GW parameterization employed (see Fritts and
 14 Alexander, 2003, for a review).

15 4. Nonlinear processes

16 For the discussion here, we classify nonlinear
 17 processes as wave–wave interactions, instability
 18 dynamics, or wave–mean flow interactions, though,
 19 as will be seen below, this is somewhat over-
 20 simplified and, depending on the scales involved, a
 21 number of processes can be viewed from more than
 22 one perspective. We will consider wave–wave
 23 interactions to include dynamics that can be
 24 described approximately by weakly nonlinear reso-
 25 nant interactions among three GWs (or more
 26 generally among GWs and vortical modes, see
 27 Mied, 1976; McComas and Bretherton, 1977; Yeh
 28 and Liu, 1981; Müller et al., 1986; Dong and Yeh,
 29 1988; Yeh and Dong, 1989; Dunkerton, 1989; Fritts
 30 and Alexander, 2003). Instability dynamics, in our
 31 discussion, include smaller-scale processes that are
 32 typically 3D, comprise “tube-like” vortex struc-
 33 tures, occur within a preferred phase of a large-
 34 amplitude GW, and arise by extracting energy from
 35 the GW through buoyancy and/or shear sources
 36 (Klostermeyer, 1991; Lombard and Riley, 1996;
 37 Fritts et al., 1996b, 1998, 2003; Sonmor and
 38 Klaassen, 1997; Fritts and Alexander, 2003). Wa-
 39 ve–mean flow interactions include the responses of
 40 the mean flow (or larger-scale motions) to GW
 41 momentum flux divergence and the mean and
 42 spatially and temporally localized body forces that
 43 arise from this divergence (Vincent and Reid, 1983;
 44 Fritts and Vincent, 1987; Zhu and Holton, 1987;
 45 Vadas and Fritts, 2001; Fritts et al., 2002). Each of
 46 these processes is discussed in greater detail below.

47 As an example of the complexity that can arise in
 48 instability studies, we show in Fig. 7 predictions of
 49 instability growth rates for various streamwise and
 50 spanwise wavenumbers (α, β) scaled by the GW total

51 wavenumber following the methodology of Lom-
 52 bard and Riley (1996). Here, “streamwise” refers to
 53 the direction of propagation of the GW, whereas
 54 “spanwise” refers to the cross-stream, or horizontal
 55 orthogonal, direction. These plots reveal that
 56 instability alignment, scales, and growth rates are
 57 all strong functions of GW amplitude, frequency,
 58 and Reynolds number and that there are, in general,
 59 multiple possible instability structures having com-
 60 parable growth rates for any combination of GW
 61 parameters. This complicates both applications of
 62 instability theory and interpretations of apparent
 63 instability structures in observed flows in the atmo-
 64 sphere and the laboratory. It also means that there
 65 may be competing instabilities (having very similar
 66 growth rates, but very different orientations, scales,
 67 and energetic sources) in any specific flow. Similar
 68 results are obtained with the methodology of
 69 Sonmor and Klaassen (1997), though their presen-
 70 tation emphasizes only those modes having the
 71 dominant growth rate at each point in parameter
 72 space. Klostermeyer (1991), Lombard and Riley
 73 (1996), and Sonmor and Klaassen (1997) all also
 74 identify links between instability structures at small
 75 and large amplitudes and other modes identified by
 76 previous authors (Hines, 1971, 1988; Yeh and Liu,
 77 1981).

78 The situation is further complicated in recogniz-
 79 ing that optimal perturbation theory (Farrell and
 80 Ioannou, 1996a, b; Achatz and Schmitz, 2004a, b)
 81 indicates that initial conditions can easily determine
 82 the dominant finite-amplitude response for flows
 83 that are nonorthonormal (i.e., eigenvectors are not
 84 orthogonal, hence any one solution is not described
 85 by a unique combination), as is the case for all
 86 sheared and stratified flows. In simple terms, a flow
 87 that does not have orthogonal eigenfunctions can
 88 experience rapid growth of arbitrary initial pertur-
 89 bations that project onto eigenfunctions having
 90 similar structures but very different growth (or
 91 decay!) rates. Indeed, the underlying flow may be
 92 stable from the perspective of traditional linear
 93 stability analysis, but nevertheless allow transitions
 94 to instability and turbulence that can only be
 95 understood from the more general optimal pertur-
 96 bation perspective.

97 4.1. Nonlinear wave–wave interactions

98 Wave–wave interactions have been explored
 99 extensively in seeking to understand spectral energy
 100 transfers and the maintenance and apparent uni-

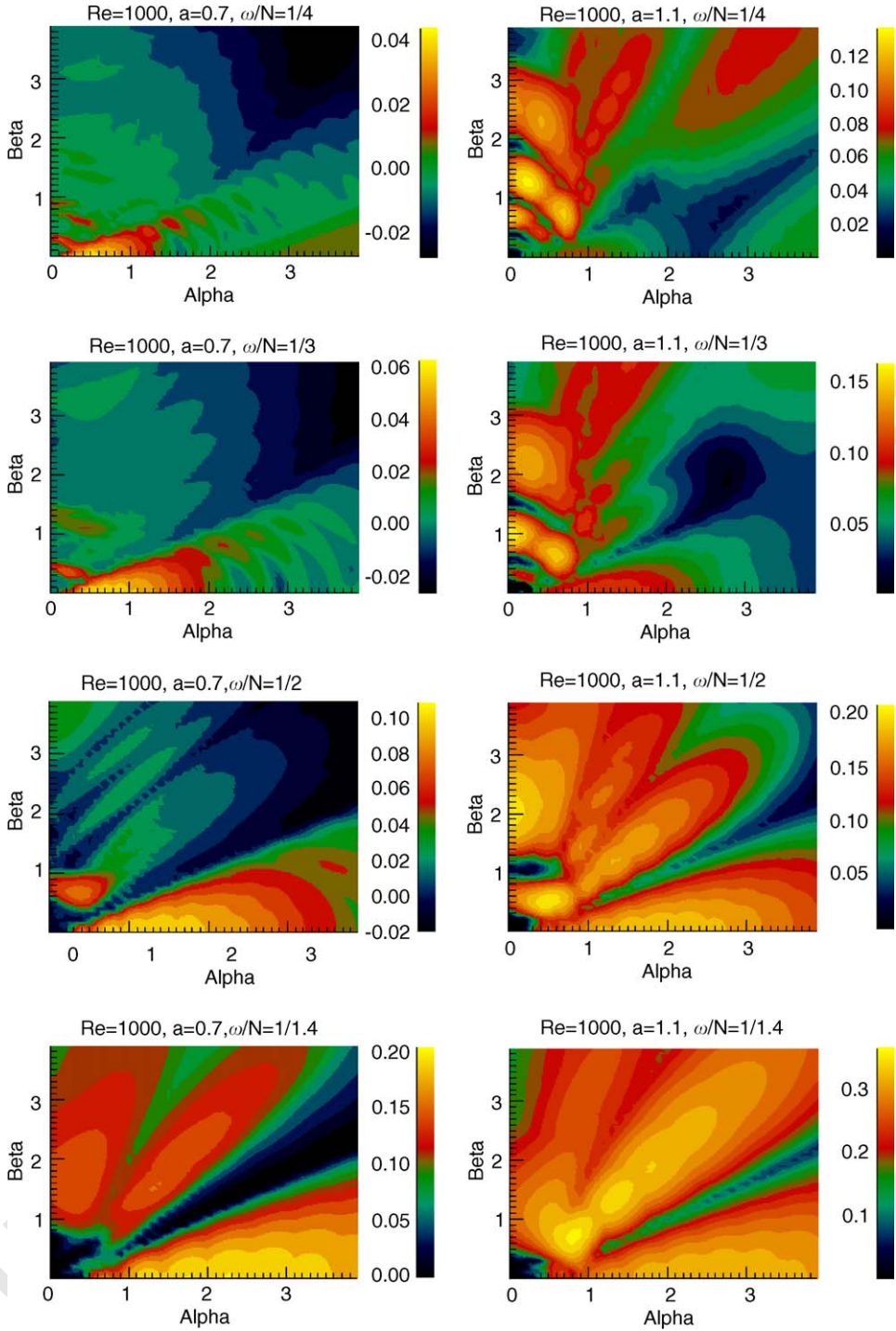


Fig. 7. Instability growth rates as a function of streamwise (α) and spanwise (β) wavenumber for GWs having $a = 0.7$ (left) and 1.1 (right) and intrinsic frequencies $\omega = N/4, N/3, N/2$, and $N/1.4$ (top to bottom) at $Re = 1000$ (after Lombard and Riley, 1996). Wavenumbers are normalized by the primary GW total wavenumber.

versality of the GW spectrum in the oceans and the atmosphere (Mied, 1976; McComas and Bretherton, 1977; Yeh and Liu, 1981; Müller et al., 1986;

Dunkerton, 1989). Generalizations to include GW–vortical mode interactions, the influences of mean shear, and the links of these “resonant” three-

53
55
57
59
61
63
65
67
69
71
73
75
77
79
81
83
85
87
89
91
93
95
97

1
3
5
7
9
11
13
15
17
19
21
23
25
27
29
31
33
35
37
39
41
43
45
47
49
51

1 wave interactions at small amplitudes to local GW
 2 instabilities at larger amplitudes have also been
 3 explored more recently (Dong and Yeh, 1988; Yeh
 4 and Dong, 1989; Klostermeyer, 1991; Vanneste,
 5 1995; Sonmor and Klaassen, 1997). It is important
 6 to recognize, however, that these and other non-
 7 linear dynamics do not occur in isolation, but as
 8 part of a continuous competition. As an example,
 9 Müller et al. (1986) examined the relevance of off-
 10 resonant or higher-order interactions in describing
 11 GW spectral energy transfers. In another, Kloster-
 12 meyer (1991) identified specific resonant interactions
 13 or instability processes across the full range of GW
 14 amplitudes, suggested that resonance dynamics may
 15 be the basis of all GW instability, and found with
 16 numerical studies that multiple interactions quickly
 17 populated the spectrum across a wide range of
 18 frequencies and wavenumbers. Finally, Thorpe
 19 (1994) found a parametric subharmonic instability
 20 (PSI) to operate effectively even at “unstable” GW
 21 amplitudes when viewed from a traditional instabil-
 22 ity perspective. Thus, wave–wave interaction dy-
 23 namics must play a central role in GW propagation,
 24 interaction, and instability dynamics, though their
 25 full impacts remain to be assessed.

26 As an example of the interactions among and
 27 competition between instability processes, we show
 28 in Fig. 8 results of a direct numerical simulation
 29 (DNS) of the evolution of a GW having an
 30 amplitude of $a = u'/(c - U) = 0.7$, well below that
 31 required for convective instability in the traditional
 32 view of GW instability (though anticipated to be
 33 unstable to wave–wave interactions in the analyses
 34 by Lombard and Riley (1996) and Sonmor and
 35 Klaassen (1997)). In this simulation, we have
 36 inclined the simulation domain along the phase of
 37 the GW, which is propagating upward and leftward
 38 (the long edge of the domain is parallel to the phase
 39 surfaces of the GW).

40 The images on the left are streamwise cross
 41 sections in the plane of propagation; those on the
 42 right are spanwise cross sections (a plane perpendi-
 43 cular to the group velocity) at the center of the
 44 slanted domain. In both set of images, bright values
 45 denote high shear or vorticity and black shades are
 46 zero shear or vorticity, and times are in units of T_b
 47 since initial conditions were posed. In the upper
 48 images, only the primary GW is apparent, as the
 49 initial noise is very small. In the second images,
 50 there is no detectable spanwise (right image)
 51 variation, but there are now significant variations
 in the streamwise structure (left image) that indicate

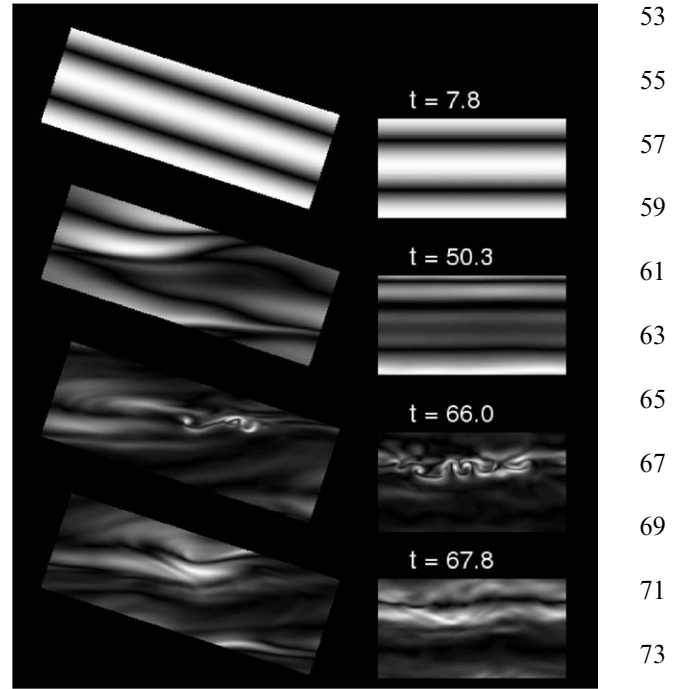


Fig. 8. A DNS of GW instability for $a = 0.7$, $Re = 3000$, and $\omega = N/3$ in a computational domain slanted along the GW phase surfaces. Time units are buoyancy periods, T_b . The dominant instability initially is a largely 2D wave–wave interaction, but increasing gradients arising from wave superposition trigger a local 3D instability thereafter. At later times, the flow is returning to a quasi-2D structure, with largely horizontal phase surfaces.

that (2D) wave–wave interactions have begun to
 play a role in the evolution. The apparent orienta-
 tion of the emerging wave structures are more
 nearly horizontal than the initial GW and are
 consistent with a PSI as initially identified by
 McComas and Bretherton (1977) and observed
 thereafter in numerical and laboratory studies by
 Klostermeyer (1991), Thorpe (1994), Vanneste
 (1995), and others. The subharmonics that arise
 (typically having larger m and smaller $|\mathbf{k}|$ than the
 initial GW) must have periodic boundary condi-
 tions in the computational domain (not multiple
 horizontal wavelengths, but subharmonics, i.e. λ/n ,
 with n an integer), but appear not strongly
 constrained by this requirement. In studies currently
 in progress, we are relaxing this constraint to
 determine whether it has restricted the form and
 growth rate of the instability.

The evolution departs sharply from a largely 2D
 flow by the third images, where we now see that the
 superposition of 2D motions having smaller vertical
 scales has led to larger gradients and local 3D

1 instability as observed in our earlier GW breaking
 2 simulations of a single wave (Andreassen et al.,
 3 1994, 1998; Fritts et al., 1994, 1996b, 1998, 2003).
 4 Indeed, the local instability structure appears to
 5 have much in common with those earlier simula-
 6 tions, especially the streamwise-aligned and coun-
 7 ter-rotating nature of the initial instability (some of
 8 this character can still be seen in the spanwise cross
 9 section at $t = 66$).

10 By the fourth images, the instability has largely
 11 disappeared, the GW amplitudes have been re-
 12 duced, and the flow has returned to a more 2D
 13 character having largely subharmonic structure.
 14 The message from this simulation, like the labora-
 15 tory study by Thorpe (1994), is that different
 16 instability dynamics can occur simultaneously, in
 17 competition with one another, or successively,
 18 depending on the structure of the large- and small-
 19 scale flows.

21 4.2. GW instability dynamics

22 Wave-wave interactions were seen above to lead
 23 to local instability as the 2D flow evolved larger
 24 gradients at smaller spatial scales. Here we show
 25 more quantitative results for a single monochro-
 26 matic GW in order to understand more fully the
 27 implications of wave breaking for GW amplitude
 28 evolution. A similar result was discussed in some
 29 detail by Fritts et al. (2003) previously. However,
 30 the present results are for a significantly higher
 31 Reynolds number and exhibit more vigorous tur-
 32 bulence extending to smaller scales of motion.

33 Streamwise and spanwise cross sections of vorticity
 34 for a simulation of GW breaking for an initial
 35 amplitude $a = 1.1$, $\omega = N/3$, and $Re = 3000$ are
 36 shown in Fig. 9. Time units, the initial noise
 37 spectrum, and the domain size are the same as in
 38 Fig. 8. The first thing to note is that instability
 39 both arises and advances much more rapidly for
 40 $a = 1.1$ than for $a = 0.7$. The first images for
 41 $a = 0.7$ in Fig. 8 show no evidence of instabil-
 42 ity, whereas the upper right (spanwise) image in
 43 Fig. 9 exhibits significant modulation within the
 44 upper region of high vorticity at about the same
 45 time. The second images shown less than a wave
 46 period later exhibit well-developed instability
 47 features having displacements extending across
 48 a significant part of the GW phase structure.
 49 The form of the instability is the same as iden-
 50 tified by Fritts et al. (2003) at a Reynolds num-
 51 ber, $Re = 1000$, comprising streamwise-aligned
 counter-rotating vortices that are largely horizontal,

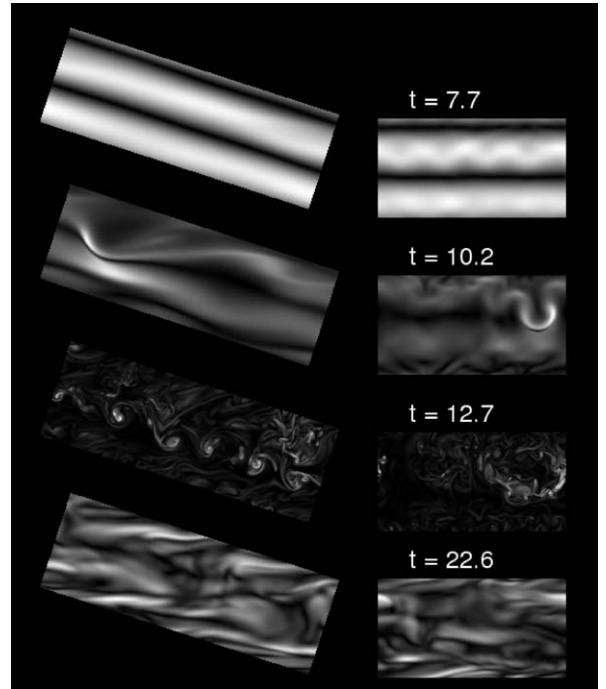


Fig. 9. As in Fig. 8, but for an initial GW amplitude of $a = 1.1$. In this case, initial instability is 3D, with counter-rotating, streamwise-aligned vortices dominating the early evolution, and vigorous turbulence arises quickly (within $\sim a$ wave period of strong initial instability). The late wave field includes the initial GW at smaller amplitude and other components having more nearly horizontal phase alignment.

largely confined to the most unstable phase of the GW, and linked by loops having largely spanwise vorticity and extending lower in the GW structure. Another $2.5T_b$ later (at $t = 12.7$), the large-scale coherent structures have been replaced by intense turbulence seeming to fill the majority of the GW field and to include a train of coherent spanwise vortices along one phase of the GW. Another $\sim 10T_b$ later, the turbulence has largely abated, and there is evidence of a residual initial GW as well as more nearly horizontal structures similar to those seen for $a = 0.7$ in Fig. 8.

The GW amplitude and heat flux throughout this evolution are shown in the left panel of Fig. 10. The amplitude is seen to drop from its initial value by more than a factor of 3 to $a \sim 0.35$, with most of this reduction occurring between the second and third images in Fig. 9. Thereafter, the amplitude (measured in the velocity field) oscillates with half the GW period due to continuing exchanges of GW energy between kinetic and potential. The heat flux computed throughout the simulation is seen to be

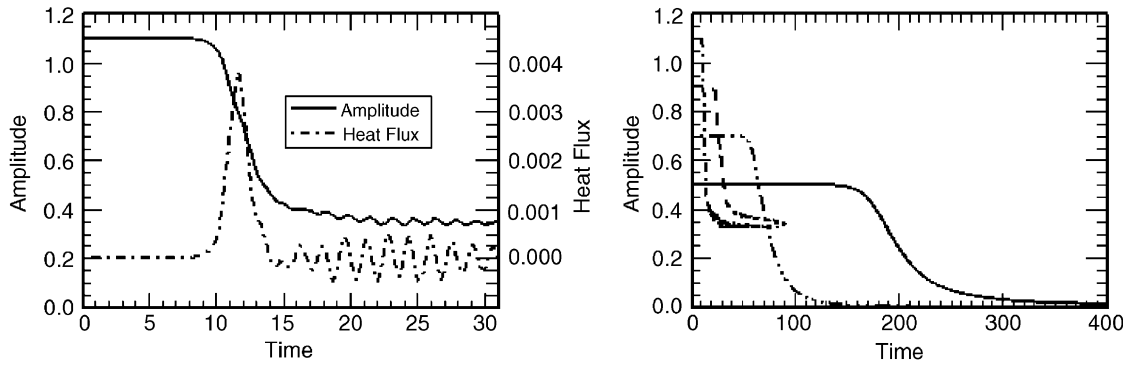


Fig. 10. Horizontal velocity amplitude, u' (left panel, solid line, left axis), and heat flux, $w'T'$, averaged over the GW phase (left panel, dashed line, right axis) throughout GW breaking for an initial amplitude of $a = 1.1$. Note that breaking and amplitude reduction occur within one GW period. Oscillations at later stages exhibit exchanges between kinetic and potential energy at a period half that of the primary GW. The right panel shows the primary GW amplitude evolution for various initial amplitudes all having $Re = 1000$ and $\omega = N/3$.

zero prior to wave breaking, to peak sharply during breaking, and to oscillate about zero again, also at half the GW period, following GW amplitude reduction and accompanying turbulence decay.

The temporal evolutions of the GW amplitudes for the two simulations discussed above, as well as for $a = 0.9$ and 0.5 , are shown together in the right panel of Fig. 10. At first glance, these results are startling. The larger initial GW amplitudes ($a = 1.1$ and 0.9) exhibit earlier and faster decay to final amplitudes of $a \sim 0.35$ or less. We earlier expressed surprise that the GW amplitude would decay so sharply relative to expectations of simple linear theory (Fritts et al., 2003). But is also surprising that an initial amplitude of $a = 0.9$ decays to an equivalent final amplitude. Even more surprising is the amplitude decay observed at smaller initial amplitudes. Indeed, these decay to zero on very long time scales. The reason is that in these cases, the decay process is wave-wave interaction rather than breaking and turbulence dissipation, and wave-wave interactions apparently transfer all of the initial GW energy to other components of the motion field on long time scales. Note, however, that while the time scale for instability at larger initial amplitudes is short and suggests that these dynamics will be important in the middle atmosphere, the time scale for wave-wave interaction is much longer. Hence these dynamics will likely play a role where vertical scales and group velocities are small, or in competition with local instability dynamics at larger amplitudes, as noted by Thorpe (1994). But they are unlikely to compete at larger group velocities with other dynamics accompanying

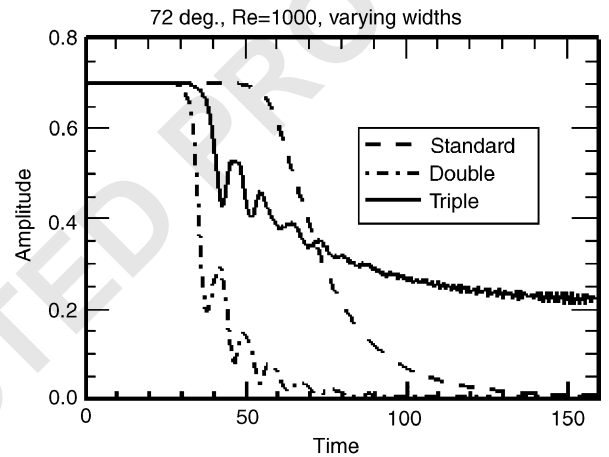


Fig. 11. GW amplitude evolutions for $a = 0.7$, $Re = 1000$, and $\omega = N/3$ for differing computational domain depths. Note that larger domains enable different and earlier instabilities, but that the apparent instability evolution and ultimate GW amplitude is a function of the allowed spatial scales (and resonant interactions).

rapid amplitude growth due to density decay with increasing altitude.

A final caveat is illustrated in Fig. 11. Displayed here are the amplitude evolutions for three simulations having an initial amplitude $a = 0.7$, and all other parameters identical except for the depth of the computational domain. To explore sensitivity to the presence of other allowed scales (and increasing degrees of freedom), we first doubled, then tripled, the domain depth. In the first case, we observed an earlier and more rapid amplitude decay than in the “standard” domain, also to a final zero amplitude, but now having amplitude oscillations of period $\sim 7T_b$, suggesting an oscillation between kinetic and

potential energy of a wave motion having a period $\sim 14T_b$. This itself is not surprising, as increasing the domain size (and degrees of freedom) allows for other possible interactions than can occur in the more confined domain. The surprising result is that when the domain depth is tripled, we obtain a dramatically different solution than for either of the smaller domains. Again, instability is advanced to an earlier time, relative to the standard domain (but not to the same degree), and initial oscillations occur suggesting the excitation of a GW having a period of $\sim 14T_b$, as in the doubled domain. In this case, however, we also see that the initial GW amplitude no longer falls to zero, but to an intermediate amplitude of $a \sim 0.22$, and that oscillations occur at \sim half the initial GW period as the amplitude stabilizes at the smaller value. This suggests that the initial wave–wave interaction was interrupted, that local instability occurred, and that the resulting drop in amplitude prevented further energy transfer by the initial wave–wave interaction. While we are working to understand these results more fully, they suggest that care must be taken in assessing instability dynamics and effects in general, and that one must be aware of possible artificial constraints on available modes of instability.

4.3. Wave–mean flow interactions

Body forcing accompanying GW dissipation and momentum flux divergence is now understood to be responsible for closure of the mesospheric jets and reversal of the meridional temperature gradient at the mesopause, to play a role in the equatorial quasi-biennial (QBO) and semiannual oscillations (SAO), and to contribute to systematic departures from geostrophic or gradient wind balance under a variety of other conditions based on over two decades of modeling, theoretical, and observational studies. At middle and high latitudes, GW momentum flux divergence contributes a mean body forcing of $\sim 50\text{--}100\text{ m s}^{-1}\text{ day}^{-1}$ near the mesopause that opposes the summer and winter mesospheric jets, alters the mean force balance, and results in a mean meridional motion of $\sim 20\text{ m s}^{-1}$ that yields a Coriolis torque that balances the zonal body force (Nastrom et al., 1982; Holton, 1982, 1983; Garcia, 1989; Fritts and Luo, 1995). Observations and theory also attribute the majority of this forcing at middle and high latitudes to GW having relatively high intrinsic frequencies due to the shape of the

frequency spectra displayed in Fig. 5 (Vincent and Reid, 1983; Fritts, 1984a; Fritts and Vincent, 1987).

The latitudinal, seasonal, and hemispheric variations of the mean GW forcing are not known well, but observations of mean meridional motions and the mean solstice thermal structure, and especially the separated mesopause, with a low, cold mesopause confined to middle and high latitudes of the summer hemisphere, offer important insights (Nastrom et al., 1982; Wang and Fritts, 1990; von Zahn et al., 1996; Lübken, 1999). Additional insights on inter-hemispheric variability in GW forcing are provided by emerging, but still controversial, lidar, radar, rocket, and satellite measurements of temperatures, winds, polar mesospheric clouds (PMC), and polar mesosphere summer echoes (PMSE) (Balsley et al., 1993, 1995; Lübken et al., 1999; Gardner et al., 2001; Bailey et al., 2004). Similar body forcing, though much smaller in magnitude, also occurs at lower altitudes, in particular the winter polar stratosphere (Hitchman et al., 1989; Garcia and Boville, 1994), and at lower latitudes, where GW momentum flux divergence contributes to the structure and variability of the QBO and SAO and is associated largely with GWs excited by deep convection across a wide range of frequencies (Dunkerton, 1982, 1997; Salby and Garcia, 1987; Bergman and Salby, 1994; Mayr et al., 1997; Baldwin et al., 2001; Pfister et al., 1993a,b; Alexander et al., 2000; Alexander and Vincent, 2000).

A useful framework from which to view the mean zonal forcing is via the “downward control principle”, which relates the Lagrangian vertical motion to the meridional gradient of the zonal body force applied to the atmosphere at higher altitudes (see McIntyre, 1989; Haynes et al., 1991; Garcia and Boville, 1994). Essentially, this describes the circulation through any level that must occur to satisfy continuity and accommodate the vertical coupling due to GWs arising in the lower atmosphere and dissipating at higher altitudes. Hence, a mean momentum flux at any altitude implies a corresponding mean vertical motion (the momentum flux must be zero at the pole) because a momentum flux divergence above requires a vertical mass flux to balance that accompanying the residual mean meridional motion providing the force balance at the altitude of GW dissipation.

Finally, recent efforts have accounted for the “missing forces” accompanying turning, or a change in GW propagation direction, in an envir-

53
55
57
59
61
63
65
67
69
71
73
75
77
79
81
83
85
87
89
91
93
95
97
99
101

1 onment having large-scale vertical vorticity. It is
 2 clear how to account for momentum transport and
 3 mean flow responses in cases where GW propaga-
 4 tion remains confined to a vertical plane. It was not
 5 obvious, however, how to account for momentum
 6 transport in cases where GW propagation direction
 7 rotates in the horizontal. This problem was ad-
 8 dressed by Bühler and McIntyre (2003, 2005), with
 9 the result that the momentum balance is just as we
 10 would have hoped: net momentum is conserved in
 11 two horizontal dimensions.

13 5. Summary and conclusions

15 A variety of measurements, modeling, and
 16 theoretical studies have provided an increasingly
 17 quantitative understanding of the mean forcing of
 18 the middle atmosphere by GWs in the last two
 19 decades. Only more recently, however, have we
 20 begun to appreciate the considerable variability of
 21 GWs and their effects at higher altitudes. This
 22 variability arises due to the inherent intermittency in
 23 GW sources, energy and momentum transports,
 24 propagation conditions, wave-wave and wave-
 25 mean flow interactions, and especially instability
 26 dynamics across the full range of GW spatial and
 27 temporal scales.

28 Mean forcing by GWs closes the mesospheric jets,
 29 induces a strong mean meridional motion, reverses
 30 the meridional temperature gradient in the upper
 31 mesosphere relative to radiative inputs, and results
 32 in a mesopause having two fairly distinct altitudes
 33 under solstice conditions. Similar, though smaller,
 34 responses also occur in the meridional (and vertical)
 35 circulation and thermal structure of the polar winter
 36 stratosphere. At lower latitudes, GWs contribute
 37 significantly to the mean structures of the QBO and
 38 SAO, with effects extending throughout the middle
 39 atmosphere.

40 GW variability also has major effects across a
 41 wide range of scales. At larger scales, these include
 42 modulation by and feedbacks on tidal and planetary
 43 wave motions and seasonal, inter-annual, and inter-
 44 hemispheric variations in mean zonal wind struc-
 45 ture, the induced residual (meridional and vertical)
 46 circulation, and the mean temperature structure. At
 47 smaller scales, GWs contribute highly variable local
 48 structure, variances, local energy and momentum
 49 fluxes, additional GW excitation, and turbulence
 50 and diffusion. Indeed, we expect that as our
 51 understanding of GW dynamics improves further,
 we will find evidence of variability (and mean

responses) extending to even higher altitudes that
 recognized at present.

Acknowledgments

Support for this research was provided by
 AFOSR under contract F49620-00-C-0045, NASA
 under contracts NAS5-02036 and NAS5-02069, and
 NSF under grants ATM-0137354, ATM-0307910,
 and ATM-0314060.

References

- Achatz, U., Schmitz, G., 2004a. Shear and convective instability of inertia-gravity wave packets: Modal and nonmodal growth. *Journal of Atmospheric Science*, submitted for publication.
- Achatz, U., Schmitz, G., 2004b. Optimal growth in convectively stable inertia-gravity wave packets: Three-dimensional structure and early nonlinear development. *Journal of Atmospheric Science*, submitted for publication.
- Alexander, M.J., Holton, J.R., Durran, D.R., 1995. The gravity wave response above deep convection in a squall line simulation. *Journal of Atmospheric Science* 52, 2212–2226.
- Alexander, M.J., Beres, J.H., Pfister, L., 2000. Tropical stratospheric gravity wave activity and relationship to clouds. *Journal of Geophysical Research* 105, 22,299–22,309.
- Alexander, M.J., Tsuda, T., Vincent, R.A., 2002. Latitudinal variations observed in gravity waves with short vertical wavelengths. *Journal of Atmospheric Science* 59, 1394–1404.
- Alexander, M.J., Vincent, R.A., 2000. Gravity waves in the tropical lower stratosphere: a model study of seasonal and interannual variability. *Journal of Geophysical Research* 105, 22299–22310.
- Allen, S.J., Vincent, R.A., 1995. Gravity wave activity in the lower atmosphere: seasonal and latitudinal variations. *Journal of Geophysical Research* 100, 1327–1350.
- Andraessen, O., Wasberg, C.-E., Fritts, D.C., Isler, J.R., 1994. Gravity wave breaking in two and three dimensions, 1. Model description and comparison of two-dimensional evolutions. *Journal of Geophysical Research* 99, 8095–8108.
- Andraessen, O., Hvidsten, P.O., Fritts, D.C., Arendt, S., 1998. Vorticity dynamics in a breaking gravity wave, 1. Initial instability evolution. *Journal of Fluid Mechanics* 367, 27–46.
- Andrews, D.G., McIntyre, M.E., 1976. Planetary waves in horizontal and vertical shear: the generalized Eliassen–Palm relation and the mean zonal acceleration. *Journal of Atmospheric Science* 33, 2031–2048.
- Bailey, S.M., Merkel, A.W., Thomas, G.E., 2004. Observations of polar mesospheric clouds by the Student Nitric Oxide Explorer. *Journal of Geophysical Research*, in press.
- Baldwin, M.P., Gray, L.J., Dunkerton, T.J., Hamilton, K., Haynes, P.H., Randel, W.J., Holton, J.R., Alexander, M.J., Hirota, I., Horinouchi, T., Jones, D.B.A., Kinnery, J.S., Marquardt, C., Sato, K., Takahashi, M., 2001. The quasi-biennial oscillation. *Reviews of Geophysics* 39, 179–229.
- Balsley, B.B., Woodman, R.F., Sarango, M., Urbino, J., Rodriguez, R., Ragaini, E., Carey, J., 1993. Southern

- 1 hemisphere PMES: where are they? *Geophysical Research Letters* 20, 1983–1985.
- 3 Balsley, B.B., Woodman, R.F., Sarango, M., Rodriguez, R.,
Urbino, J., Ragaini, E., Carey, J., Huaman, J., Giraldez, A.,
5 1995. On the lack of southern-hemisphere PMSE. *Journal of Geophysical Research* 100, 11685–11693.
- 7 Bergman, J.W., Salby, M.L., 1994. Equatorial wave activity derived from fluctuations in observed convection. *Journal of Atmospheric Science* 51, 3791–3806.
- 9 Broutman, D., 1986. On internal wave caustics. *Journal of Physical Oceanography* 16, 1625–1635.
- 11 Broutman, D., Young, W.R., 1986. On the interaction of small-scale internal waves with near-inertial waves. *Journal of Fluid Mechanics* 166, 341–358.
- 13 Broutman, D., MacCaskill, C., McIntyre, M.E., Rottman, J.W., 1997. On Doppler spreading models of internal waves. *Geophysical Research Letters* 24, 2813–2816.
- 15 Broutman, D., Rottman, J.W., Eckermann, S.D., 2002. Maslov's method for stationary hydrostatic mountain waves. *Quarterly Journal of Royal Meteorological Society* 128, 1159–1172.
- 17 Broutman, D., Rottman, J.W., Eckermann, S.D., 2003. A simplified Fourier method for nonhydrostatic mountain waves. *Journal of Atmospheric Science* 60, 2686–2696.
- 19 Broutman, D., Rottman, J.W., Eckermann, S.D., 2004. Ray methods for internal waves in the atmosphere and ocean. *Annual Review on Fluid Mechanics* 36, 233–253.
- 21 Bruhwiler, D.L., Kaper, T.J., 1995. Wavenumber transport: scattering of small-scale internal waves by large-scale wavepackets. *Journal of Fluid Mechanics* 289, 379–405.
- 23 Buckley, G., Broutman, D., Rottman, J.W., Eckermann, S., 1999. On the importance of weak steady shear in the refraction of short internal waves. *Geophysical Research Letters* 26, 2877–2880.
- 25 Bühler, O., McIntyre, M.E., 1999. On shear generated gravity waves that reach the mesosphere, part II: Wave propagation. *Journal of Atmospheric Science* 56, 3764–3773.
- 27 Bühler, O., McIntyre, M.E., 2003. Remote recoil: a new wave–mean interaction effect. *Journal of Fluid Mechanics* 492, 207–230.
- 29 Bühler, O., McIntyre, M.E., 2005. Wave capture and wave-vortex duality. *Journal of Fluid Mechanics*, submitted for publication.
- 31 Bühler, O., McIntyre, M.E., Scinocca, J.F., 1999. On shear generated gravity waves that reach the mesosphere, part I: Wave generation. *Journal of Atmospheric Science* 56, 3749–3763.
- 33 Chimonas, G., Grant, J.R., 1984. Shear excitation of gravity waves. Part II: upscale scattering from Kelvin–Helmholtz waves. *Journal of Atmospheric Science* 41, 2278–2288.
- 35 Clark, T.L., Hauf, T., Kuettner, J.P., 1986. Convectively forced internal gravity waves: results from two-dimensional numerical experiments. *Quarterly Journal of Royal Meteorological Society* 112, 899–925.
- 37 Dewan, E.M., Picard, R.H., O'Neil, R.R., Gardiner, H.A., Gibson, J., Mill, J.D., Richards, E., Kendra, M., Gallery, W.O., 1998. MSX satellite observations of thunderstorm-generated gravity waves in mid-wave infrared images of the upper Stratosphere. *Geophysical Research Letters* 25, 939–942.
- 39 Dong, B., Yeh, K.C., 1988. Resonant and nonresonant wave–wave interactions in an isothermal atmosphere. *Journal of Geophysical Research* 93, 3729–3744.
- Dunkerton, T.J., 1982. Theory of the mesopause semiannual oscillation. *Journal of Atmospheric Science* 39, 2681–2690.
- Dunkerton, T.J., 1987. Effect of nonlinear instability on gravity wave momentum transport. *Journal of Atmospheric Science* 44, 3188–3209.
- Dunkerton, T.J., 1989. Theory of internal gravity wave saturation. *Pure and Applied Geophysics* 130, 373–397.
- Dunkerton, T.J., 1997. The role of gravity waves in the quasi-biennial oscillation. *Journal of Geophysical Research* 102, 26053–26076.
- Eckermann, S.D., 1997. Influence of wave propagation on the Doppler-spreading of atmospheric gravity waves. *Journal of Atmospheric Science* 54, 2554–2573.
- Farrell, B.F., Ioannou, P.J., 1996a. Generalized stability theory. Part I: autonomous operators. *Journal of Atmospheric Science* 53, 2025–2040.
- Farrell, B.F., Ioannou, P.J., 1996b. Generalized stability theory. Part II: nonautonomous operators. *Journal of Atmospheric Science* 53, 2041–2053.
- Fetzer, E.J., Gille, J.C., 1994. Gravity wave variance in LIMS temperatures. Part I. Variability and comparison with background winds. *Journal of Atmospheric Science* 51, 2461–2483.
- Fetzer, E.J., Gille, J.C., 1996. Gravity wave variance in LIMS temperatures. Part II: Comparison with the zonal-mean momentum balance. *Journal of Atmospheric Science* 53, 398–410.
- Fovell, R., Durran, D., Holton, J.R., 1992. Numerical simulations of convectively generated stratospheric gravity waves. *Journal of Atmospheric Science* 49, 1427–1442.
- Fritts, D.C., 1984a. Gravity wave saturation in the middle atmosphere: a review of theory and observations. *Review of Geophysics and Space Physics* 22, 275–308.
- Fritts, D.C., 1984b. Shear excitation of atmospheric gravity waves. Part II: nonlinear radiation from a free shear layer. *Journal of Atmospheric Science* 41, 524–537.
- Fritts, D.C., 1989. A review of gravity wave saturation processes, effects, and variability in the middle atmosphere. *Pure and Applied Geophysics* 130, 343–371.
- Fritts, D.C., Alexander, M.J., 2003. Gravity dynamics and effects in the middle atmosphere. *Reviews of Geophysics* 41.
- Fritts, D.C., Luo, Z., 1992. Gravity wave excitation by geostrophic adjustment of the jet stream, Part I: two-dimensional forcing. *Journal of Atmospheric Science* 49, 681–697.
- Fritts, D.C., Luo, Z., 1995. Dynamical and radiative forcing of the summer mesopause circulation and thermal structure, 1. Mean Solstice conditions. *Journal of Geophysical Research* 100, 3119–3128.
- Fritts, D.C., Nastrom, G.D., 1992. Sources of mesoscale variability of gravity waves, II: frontal, convective, and jet stream excitation. *Journal of Atmospheric Science* 49, 111–127.
- Fritts, D.C., VanZandt, T.E., 1987. Effects of Doppler shifting on the frequency spectra of atmospheric gravity waves. *Journal of Geophysical Research* 92, 9723–9732.
- Fritts, D.C., VanZandt, T.E., 1993. Spectral estimates of gravity wave energy and momentum fluxes, I: energy dissipation, acceleration, and constraints. *Journal of Atmospheric Science* 50, 3685–3694.
- Fritts, D.C., Vincent, R.A., 1987. Mesospheric momentum flux studies at Adelaide, Australia: observations and a gravity

- 1 wave/tidal interaction model. *Journal of Atmospheric Science* 44, 605–619.
- 3 Fritts, D.C., Isler, J.R., Andreassen, O., 1994. Gravity wave
breaking in two and three dimensions, 2. Three-dimensional
5 evolution and instability structure. *Journal of Geophysical
Research* 99, 8109–8123.
- 7 Fritts, D.C., Palmer, T.L., Andreassen, O., Lie, I., 1996a.
Evolution and breakdown of Kelvin–Helmholtz billows in
9 stratified compressible flows, I: comparison of two- and three-
dimensional flows. *Journal of Atmospheric Science* 53,
3173–3191.
- 11 Fritts, D.C., Garten, J.F., Andreassen, O., 1996b. Wave breaking
and transition to turbulence in stratified shear flows. *Journal
of Atmospheric Science* 53, 1057–1085.
- 13 Fritts, D.C., Arendt, S., Andreassen, O., 1998. Vorticity
dynamics in a breaking internal gravity wave, 2. Vortex
15 interactions and transition to turbulence. *Journal of Fluid
Mechanics* 367, 47–65.
- 17 Fritts, D.C., Vadas, S.A., Yamada, Y., 2002. An estimate of
strong local gravity wave body forcing based on OH airglow
19 and meteor radar observations. *Geophysical Research Letters*
29 (10), 1.
- 21 Fritts, D.C., Bizon, C., Werne, J.A., Meyer, C.K., 2003. Layering
accompanying turbulence generation due to shear instability
and gravity wave breaking. *Journal of Geophysical Research*
108 (D8), 8452.
- 23 Garcia, R.R., 1989. Dynamics, radiation, and photochemistry in
the mesosphere: implications for the formation of noctilucent
25 clouds. *Journal of Geophysical Research* 94, 14,605–14,615.
- 27 Garcia, R.R., Boville, B., 1994. “Downward control” of the
mean meridional circulation and temperature distribution of
the polar winter stratosphere. *Journal of Atmospheric Science*
51, 2238–2245.
- 29 Garcia, R.R., Sassi, F., 1999. Modulation of the Mesospheric
Semiannual Oscillation by the Quasi-biennial Oscillation.
31 *Earth Planets Space* 51, 563–569.
- 33 Gardner, C.S., Papan, G.C., Chu, X., Pan, W., 2001. First lidar
observations of middle atmosphere temperatures, Fe densi-
ties, and polar mesospheric clouds over the North and South
35 Poles. *Geophysical Research Letters* 28, 1199–1202.
- 37 Griffiths, M., Reeder, M.J., 1996. Stratospheric inertia-gravity
waves generated in a numerical model of frontogenesis. I:
model solutions. *Quarterly Journal of Royal Meteorological
Society* 122, 1153–1174.
- 39 Haynes, P.H., Marks, C.J., McIntyre, M.E., Shephard, T.G.,
Shine, K.P., 1991. On the “Downward Control” of extra-
tropical diabatic circulations by eddy-induced mean zonal
41 forces. *Journal of Atmospheric Science* 48, 657–678.
- 43 Hecht, J.H., Liu, A.Z., Walterscheid, R.L., Rudy, R.J., 2004.
Maui Mesosphere and Lower Thermosphere (Maui MALT)
observations of the evolution of Kelvin–Helmholtz billows
45 formed near 86 km altitude. *Journal of Geophysical Research*,
109, D22S10, doi:10.1029/2003JD003908, in press.
- 47 Hertzog, A., Vial, F., 2001. A study of the dynamics of the
equatorial lower atmosphere by use of ultra-long duration
balloons, 2, gravity waves. *Journal of Geophysical Research*
106, 22,745–22,761.
- 49 Hines, C.O., 1971. Generalizations of the Richardson criterion
for the onset of atmospheric turbulence. *Quarterly Journal of
Royal Meteorological Society* 97, 429–439.
- 51 Hines, C.O., 1988. The generation of turbulence by atmospheric
gravity waves. *Journal of Atmospheric Science* 45, 1269–1278.
- Hitchman, M.H., Gille, J.C., Rodgers, C.D., Brasseur, G., 1989. 53
The separated polar winter stratopause: a gravity wave driven
climatological feature. *Journal of Atmospheric Science* 46, 55
410–422.
- Holton, J.R., 1982. The role of gravity wave induced drag and 57
diffusion in the momentum budget of the mesosphere. *Journal
of Atmospheric Science* 39, 791–799.
- Holton, J.R., 1983. The influence of gravity wave breaking on the 59
general circulation of the middle atmosphere. *Journal of
Atmospheric Science* 40, 2497–2507.
- 61 Horinouchi, T., Nakamura, T., Kosaka, J., 2002. Convectively
generated mesoscale gravity waves simulated throughout the
middle atmosphere. *Geophysical Research Letters* 21, 1. 63
- Isler, J.R., Fritts, D.C., 1996. Gravity wave variability and 65
interaction with lower-frequency motions in the mesosphere
and lower thermosphere over Hawaii. *Journal of Atmospheric
Science* 53, 37–48.
- Jiang, J.H., Wu, D.L., Eckermann, S.D., 2002. Upper Atmo- 67
sphere Research Satellite (UARS) MLS observation of
mountain waves over the Andes. *Journal of Geophysical
Research* 107 (D20), 1. 69
- Jiang, J.H., Wu, D.L., Eckermann, S.D., Ma, J., 2003. Mountain 71
waves in the middle atmosphere: microwave limb sounder
observations and analyses. *Advances in Space Research* 32
(5), 801–806. 73
- Jiang, J.H., Eckermann, S.D., Wu, D.L., Ma, J., 2004. A search 75
for mountain waves in MLS stratospheric limb radiance from
the Northern Hemisphere: data analysis and global mountain
wave modeling. *Journal of Geophysical Research* 109,
D03107. 77
- Karoly, D.J., Roff, G.L., Reeder, M.J., 1996. Gravity wave 79
activity associated with tropical convection detected in TOGA
COARE sounding data. *Geophysical Research Letters* 23,
261–264. 81
- Kim, Y.-J., Eckermann, S.D., Chun, H.-Y., 2003. A overview of 83
the past, present and future of gravity-wave drag parameter-
ization for numerical climate and weather prediction models.
Atmosphere-Ocean 41, 65–98.
- Klostermeyer, J., 1991. Two- and three-dimensional parametric 85
instabilities in finite amplitude internal gravity waves.
Geophysical and Astrophysical Fluid Dynamics 64, 1–25. 87
- Lane, T.P., Clark, T.L., 2002. Gravity waves generated by the dry 87
convective boundary layer: two-dimensional scale selection
and boundary layer feedback. *Quarterly Journal of Royal
Meteorological Society* 128, 1543–1570. 89
- Lane, T.P., Reeder, M.J., Clark, T.L., 2001. Numerical modeling 91
of gravity wave generation by deep tropical convection.
Journal of Atmospheric Science 58, 1249–1274.
- Lighthill, J., 1978. *Waves in Fluids*. Cambridge University Press, 93
Cambridge 504pp.
- Lombard, P.N., Riley, J.J., 1996. Instability and breakdown of 95
internal gravity waves. I. Linear stability analysis. *Physics of
Fluids* 8, 3271–3287.
- Lübken, F.-J., 1999. Thermal structure of the Arctic summer 97
mesosphere. *Journal of Geophysical Research* 104,
9135–9149. 99
- Lübken, F.-J., Jarvis, M.J., Jones, G.O.L., 1999. First in situ 101
temperature measurements at the Antarctic summer meso-
pause. *Geophysical Research Letters* 26, 3581–3584.
- Luo, Z., Fritts, D.C., 1993. Gravity wave excitation by 103
geostrophic adjustment of the jet stream, Part II: three-

- 1 dimensional forcing. *Journal of Atmospheric Science* 50, 104–115.
- 3 Manson, A.H., Meek, C.E., Hall, G.E., 1998. Correlations of
gravity waves and tides in the mesosphere over Saskatoon.
5 *Journal of Atmospheric and Solar-Terrestrial Physics* 60,
1089–1107.
- 7 Mayr, H.G., Mengel, J.G., Hines, C.O., Chan, K.L., Arnold,
N.F., Reddy, C.A., Porter, H.S., 1997. The gravity wave
9 Doppler spread theory applied in a numerical spectral model
of the middle atmosphere 2. Equatorial oscillations. *Journal*
11 *of Geophysical Research* 102, 26,093–26,105.
- 13 McComas, C.H., Bretherton, F.P., 1977. Resonant interaction of
oceanic internal waves. *Journal of Geophysical Research* 82,
1397–1412.
- 15 McIntyre, M.E., 1989. On dynamics and transport near the polar
mesopause in summer. *Journal of Geophysical Research* 94,
14,617–14,628.
- 17 McIntyre, M.E., 2003. In: Holton, J.R., Pyle, J.A., Curry, J.A.
(Eds.), *Balanced Flow, Encyclopedia of Atmospheric*
19 *Sciences*, vol. 2. Academic Press, New York, pp. 680–685.
- 21 Mied, R.P., 1976. The occurrence of parametric instabilities in
finite amplitude internal gravity waves. *Journal of Fluid*
23 *Mechanics* 78, 763–784.
- 25 Müller, P., Holloway, G., Henyey, F., Pomphrey, N., 1986.
Nonlinear interactions among internal gravity waves. *Reviews*
27 *of Geophysics* 24, 493–536.
- 29 Nakamura, T., Fritts, D.C., Isler, J.R., Tsuda, T., Vincent, R.A.,
1997. Short-period fluctuations of the diurnal tide observed
with low-latitude MF and meteor radars during CADRE:
evidence for gravity wave/tidal interactions. *Journal of*
31 *Geophysical Research* 102, 26,225–26,238.
- 33 Nastrom, G.D., Balsley, B.B., Carter, D.A., 1982. Mean
meridional winds in the mid- and high-latitude summer
35 mesosphere. *Geophysical Research Letters* 9, 139–142.
- 37 Nastrom, G.D., VanZandt, T.E., Warnock, J.M., 1997. Vertical
wavenumber spectra of wind and temperature from high-
39 resolution balloon soundings in the lower atmosphere over
Illinois. *Journal of Geophysical Research* 102, 6685–6702.
- 41 Palmer, T.L., Fritts, D.C., Andreassen, O., 1996. Evolution and
breakdown of Kelvin–Helmholtz billows in stratified com-
43 pressible flows, II: instability structure, evolution, and
energetics. *Journal of Atmospheric Science* 53, 3192–3212.
- 45 Pfister, L., Starr, W., Craig, R., Loewenstein, M., 1986. Small-
scale motions observed by aircraft in the tropical lower
47 stratosphere: evidence for mixing and its relationship to large-
scale flows. *Journal of Atmospheric Science* 43, 3210–3225.
- 49 Pfister, L., Scott, S., Loewenstein, M., Bowen, S., Legg, M.,
1993a. Mesoscale disturbances in the tropical stratosphere
excited by convection: observations and effects on the
stratospheric momentum budget. *Journal of Atmospheric*
51 *Science* 50, 1058–1075.
- Pfister, L., Chan, K.R., Bui, T.P., Bowen, S., Legg, M., Gary, B.,
Kelly, K., Proffitt, M., Starr, W., 1993b. Gravity waves
generated by a tropical cyclone during the STEP tropical field
program: a case study. *Journal of Geophysical Research* 98,
8611–8638.
- Piani, C., Durran, D., Alexander, M.J., Holton, J.R., 2000. A
numerical study of three-dimensional gravity waves triggered
by deep tropical convection and their role in the dynamics of
the QBO. *Journal of Atmospheric Science* 57, 3689–3702.
- Reeder, M.J., Griffiths, M., 1996. Stratospheric inertia-gravity
waves generated in a numerical model of frontogenesis. II:
wave sources and generation mechanisms. *Quarterly Journal*
53 *of Royal Meteorological Society* 122, 1175–1195.
- Salby, M.L., Garcia, R.R., 1987. Transient response to localized
55 episodic heating in the tropics. Part I: excitation and short-
time near-field behaviour. *Journal of Atmospheric Science* 44,
57 458–498.
- Scinocca, J.F., Ford, R., 2000. The nonlinear forcing of large-
scale internal gravity waves by stratified shear instability. *Journal*
59 *of Atmospheric Science* 57, 653–672.
- Sentman, D.D., Wescott, E.M., Picard, R.H., Winick, J.R.,
Stenbaek-Nielsen, H.C., Dewan, E.M., Moudry, D.R., São
61 Sabbas, F.T., Heavner, M.J., 2003. Simultaneous observation
of mesospheric gravity waves and sprites generated by a
63 Midwestern thunderstorm. *Journal of Atmospheric and*
Solar-Terrestrial Physics 65, 537–550.
- 65 Shimizu, A., Tsuda, T., 1997. Characteristics of Kelvin waves and
gravity waves observed with radiosondes over Indonesia.
67 *Journal of Geophysical Research* 102, 26159–26171.
- Smith, A.K., 1996. Longitudinal variations in mesospheric winds:
evidence for gravity wave filtering by planetary waves. *Journal*
69 *of Atmospheric Science* 53, 1156–1173.
- Song, I.-S., Chun, H.-Y., Lane, P.P., 2003. Generation mecha-
71 nisms of convectively forced internal gravity waves and their
propagation to the stratosphere. *Journal of Atmospheric*
73 *Science* 60, 1960–1980.
- Sonmor, L.J., Klaassen, G.P., 1997. Toward a unified theory of
75 gravity wave stability. *Journal of Atmospheric Science* 54,
2655–2680.
- Sonmor, L.J., Klaassen, G.P., 2000. Mechanisms of gravity wave
77 focusing in the middle atmosphere. *Journal of Atmospheric*
Science 57, 493–510.
- Sutherland, B.R., 1999. Propagation and reflection of internal
79 waves. *Physics of Fluids* 11, 1081–1090.
- Sutherland, B.R., 2000. Internal wave reflection in uniform shear.
81 *Quarterly Journal of Royal Meteorological Society* 126,
3255–3287.
- Sutherland, B.R., 2001. Finite-amplitude internal wavepacket
83 dispersion and breaking. *Journal of Fluid Mechanics* 429,
343–380.
- 85 Taylor, M.J., Hapgood, M.A., 1988. Identification of a thunder-
storm as a source of short period gravity waves in the upper
87 atmospheric nightglow emissions. *Planetary and Space*
Science 36, 975.
- Thayaparan, T., Hocking, W.K., MacDougall, J., 1995. Ob-
89 servational evidence of tidal/gravity wave interactions using
the UWO 2MHz radar. *Geophysical Research Letters* 22,
91 373–376.
- Thorpe, S.A., 1994. Observations of parametric instability and
93 breaking waves in an oscillating tilted tube. *Journal of Fluid*
Mechanics 261, 33–45.
- Tsuda, T., Murayama, Y., Wiryosumarto, H., Harijono, S.W.B.,
95 Kato, S., 1994. Radiosonde observations of equatorial
atmosphere dynamics over Indonesia, 2, characteristics of
97 gravity waves. *Journal of Geophysical Research* 99,
10,507–10,516.
- Tsuda, T., VanZandt, T.E., Mizumoto, M., Kato, S., Fukao, S.,
99 1991. Spectral analysis of temperature and Brunt-Vaisala
frequency fluctuations observed by radiosondes. *Journal of*
101 *Geophysical Research* 96, 17265–17278.
- Tsuda, T., Nishida, M., Rocken, C., 2000. A global morphology
103 of gravity wave activity in the stratosphere revealed by the

- 1 GPS occultation data (GPS/MET). *Journal of Geophysical Research* 105, 7257–7274.
- 3 Vadas, S.L., Fritts, D.C., 2001. Gravity wave radiation and mean responses to local body forces in the atmosphere. *Journal of Atmospheric Science* 58, 2249–2279.
- 5 Vadas, S.L., Fritts, D.C., 2002. The importance of spatial variability in the generation of secondary gravity waves from local body force s. *Geophysical Research Letters* 29 (20).
- 7 Vadas, S.L., Fritts, D.C., 2004. Thermospheric responses to gravity waves arising from mesoscale convective complexes. *Journal of Atmospheric and Solar-Terrestrial Physics* 66, 781–804.
- 9 Vadas, S.L., Fritts, D.C., Alexander, M.J., 2003. Mechanism for the generation of secondary waves in wave breaking regions. *Journal of Atmospheric Science* 60, 194–214.
- 11 Vanneste, J., 1995. The instability of internal gravity waves to localized disturbances. *Annals of Geophysics* 13, 196–210.
- 13 VanZandt, T.E., 1982. A universal spectrum of buoyancy waves in the atmosphere. *Geophysical Research Letters* 9, 575–578.
- 15 Vincent, R.A., Alexander, M.J., 2000. Gravity waves in the tropical lower stratosphere: An observational study of seasonal and interannual variability. *Journal of Geophysical Research* 105, 17971–17982.
- 17 Vincent, R.A., Reid, I.M., 1983. HF Doppler measurements of mesospheric momentum fluxes. *Journal of Atmospheric Science* 40, 1321–1333.
- 19 von Zahn, U., Höffner, J., Eska, V., Alpers, M., 1996. The mesopause altitude: only two distinctive levels worldwide? *Geophysical Research Letters* 23, 3231–3234.
- 21 Wada, K., Nitta, T., Sato, K., 1999. Equatorial inertia-gravity waves in the lower stratosphere revealed by TOGA-COARE IOP data. *Journal of Meteorological Society, Japan* 77, 721–736.
- 23 Walterscheid, R.L., 1981. Inertio-gravity wave induced accelerations of mean flow having an imposed periodic component: Implications for tidal observations in the meteor region. *Journal of Geophysical Research* 86, 9698–9706. 31
- 25 Walterscheid, R.L., 2000. Propagation of small-scale gravity waves through large-scale internal wave fields: Eikonal effects at low-frequency approximation critical levels. *Journal of Geophysical Research* 105, 18027–18037. 33
- 27 Wang, D.-Y., Fritts, D.C., 1990. Mesospheric momentum fluxes observed by the MST radar at Poker Flat, Alaska. *Journal of Atmospheric Science* 47, 1511–1521. 35
- 29 Wang, D.-Y., Fritts, D.C., 1991. Evidence of gravity wave–tidal interaction observed near the summer mesopause at Poker Flat, Alaska. *Journal of Atmospheric Science* 48, 572–583. 37
- 31 Werne, J., Fritts, D.C., 1999. Stratified shear turbulence: evolution and statistics. *Geophysical Research Letters* 26, 439–442. 39
- 33 Yamada, Y., Fukunishi, H., Nakamura, T., Tsuda, T., 2001. Breakdown of small-scale quasi-stationary gravity wave and transition to turbulence observed in OH airglow. *Geophysical Research Letters* 28, 2153–2156. 41
- 35 Yeh, K.C., Dong, B., 1989. The nonlinear interaction of a gravity wave with the vortical modes. *Journal of Atmospheric and Terrestrial Physics* 51, 45–50. 43
- 37 Yeh, K.C., Liu, C.H., 1981. The instability of atmospheric gravity waves through wave–wave interactions. *Journal of Geophysical Research* 86, 9722–9728. 45
- 39 Zhong, L., Sonmor, L.J., Manson, A.H., Meek, C.E., 1995. The influence of time-dependent wind on gravity-wave propagation in the middle atmosphere. *Annales Geophysicae* 13, 375–394. 47
- 41 Zhu, X., Holton, J.R., 1987. Mean fields induced by local gravity-wave forcing in the middle atmosphere. *Journal of Atmospheric Science* 44, 620–630. 49
- 43 51
- 45 53
- 47 55